International Journal of Digital Technology Driven Engineering, Vol. 1 No. 1 (2026), Article 003

ESN Publishing

Contents lists available at ESN Publishing Journals

International Journal of Digital Technology Driven Engineering

journal homepage: https://journals.esn-press.com/ijdtde

Research Article

Robustness-Informed Seismic Retrofit Assessment of Existing Reinforced-Concrete and Stone-Masonry Buildings under Local Element Loss

Chara Ch. Mitropoulou[1,*], Matilda Kouramanou[2], Maria Dagalaki[2], and Maria Gkara[3]

[1] *Research and Development Department, Infersence Ltd., Bakou 1, 11524 Athens, Greece*
[2] *VELTION-Engineering Optimization & Applied Machine Learning Group (http://veltion.ntua.gr/), Institute of Structural Analysis & Antiseismic Research, Department of Structural Engineering, School of Civil Engineering, National Technical University of Athens, 9, Iroon Polytechniou Str., Zografou, Athens, 15780, Attica, Greece*
[3] *Research and Development Department, Innovasphere Ltd., 92B Hristo Botev Blvd., 4000 Plovdiv, Bulgaria*

ARTICLE INFO

Article type:
Research Article

Keywords:
Structural robustness; Progressive collapse; Seismic retrofit; Reinforced concrete; Stone masonry; Alternate load path

ABSTRACT

Seismic retrofit strategies are usually evaluated for the intact structure, even though the resulting changes in strength, stiffness, and load paths may also affect performance after local damage. This study presents a unified numerical framework for examining both objectives through two contrasting case studies: a six-storey reinforced-concrete (RC) frame and a load-bearing stone-masonry building. The existing RC building was assessed by nonlinear static pushover analysis under uniform and modal lateral-load patterns. Deficient members were strengthened with RC jackets, and the retrofitted structure was then examined after the notional removal of a ground-storey column. For the masonry building, three intervention schemes were considered: mortar-joint repair with shotcrete jackets (M1), mortar-joint repair with grout injection (M2), and mortar-joint repair combined with an RC ring beam and vertical prestressing (M3). Their seismic response was compared before four local wall-removal scenarios were evaluated using normal-stress and in-plane shear criteria. In the RC case, jacketing reduced the reported number of Life-Safety exceedances from 15 to 0; the reported performance-point target displacements also decreased, while base shear increased in the two Y cases and decreased in the two X cases. Because complete capacity curves were unavailable, the mixed performance-point base-shear changes were not interpreted as evidence of increased initial stiffness or ultimate resistance. Beam strengthening around the removed support was examined qualitatively as a means of improving the alternative load path. In the masonry case, M2 produced the largest nominal reduction in the selected elastic response measures under the adopted response spectrum. Under the adopted equivalent-continuum shell model, M1 and M2 remained below the source-study shear DCR threshold in all four examined scenarios, whereas M3 exceeded that threshold in every scenario. The results show that reduced intact-state response measures do not necessarily imply greater robustness. Retrofit selection should therefore include explicit assessment of damaged configurations and of the modelled response features governing demand after local element loss.

* Corresponding author. E-mail address: chara.mitropoulou@gmail.com.
Received 1 August 2026; Revised 24 August 2026; Accepted 24 August 2026

1 Introduction

A large share of the building stock in seismic regions predates current provisions for ductile detailing, capacity design, and robustness. In such buildings, low or uncertain material strength is often accompanied by irregular geometry, weak connections, deterioration, and undocumented alterations. An earthquake assessment can reveal many of these weaknesses, but it does not answer every safety question. If a column, wall pier, or other load-bearing component is lost because of impact, fire, explosion, or construction error, the vertical loads carried by that component must find another path. Compliance with an intact-state seismic target does not, by itself, demonstrate that such a path exists.

Seismic assessment and robustness assessment ask different questions of the same structure. The seismic problem is normally posed for the intact building: calculated deformations, damage states, and member demands are checked against the limits associated with a selected performance objective. In existing reinforced-concrete (RC) buildings, nonlinear static analysis is widely used for this purpose because a single analysis sequence can provide the capacity curve, target displacement, order of hinge formation, and acceptance state of individual members [1, 2, 3, 4]. The appropriate procedure for a masonry building depends more strongly on the available construction data and on how explicitly cracking and wall interaction are to be represented; response-spectrum, time-history, and nonlinear approaches are all used in practice [3, 5]. A robustness check instead assumes that local damage has already occurred. It examines whether the structure that remains can carry the redistributed loads without allowing failure to spread beyond the initially affected region [6, 7, 8, 9]. Notional removal of a column or wall segment is a direct way of testing this residual load-transfer capacity without tying the analysis to one accidental hazard [10, 11].

This difference becomes important during retrofit design. An RC jacket raises column resistance and improves confinement, but the accompanying increase in stiffness may also attract additional force or shift demand to neighbouring members. After a column is removed, the response may depend less on the upgraded column than on the beams and connections that must bridge the unsupported bay. The same concern arises in masonry, although the mechanisms are different. Mortar-joint repair and grout injection modify the effective strength and stiffness of the wall, while jackets, ring beams, and prestressing change restraint, mass, connectivity, or the initial compression field. Their benefits under earthquake loading cannot therefore be assumed to carry over unchanged to a damaged configuration. The altered wall or frame must still be able to develop a continuous and sufficiently deformable replacement load path.

Previous progressive-collapse studies show that this response is governed by more than the nominal resistance of the removed component. Load redistribution, dynamic amplification, connection continuity, slab participation, membrane action, and the adopted failure criterion can all influence the predicted outcome [9, 8]. For RC construction, these effects have been investigated through removed-column experiments, beam–column subassemblies, floor-system models, infill-wall studies, and assessments of strengthening measures [12, 13, 14, 15, 16]. Far less evidence is available for load-bearing masonry, particularly for walls that have already been repaired or strengthened before local loss occurs. This imbalance also helps explain why cross-material studies remain rare. RC frames and masonry walls require different response quantities and failure checks, but their residual performance ultimately relies on the same system-level attributes: continuity, redundancy, and a credible route for transferring load around the damaged region.

Recent studies have addressed important parts of the relationship between structural retrofitting and progressive-collapse resistance, although mostly within individual structural typologies or for retrofit measures developed specifically for one response objective. Scalvenzi et al. [17] investigated a four-storey RC frame designed primarily for gravity loads and assessed its seismic response by nonlinear static analysis and its robustness through pushdown analyses following central- and corner-column removal. Their study showed that CFRP-based shear strengthening intended to prevent brittle failures could improve both seismic safety and progressive-collapse resistance. The investigation, however, was restricted to an RC frame, a single family of strengthening measures, and did not examine whether the relative effectiveness of different seismic retrofit alternatives changes when damaged configurations are considered. Zhang et al. [18] addressed the tension more directly at the RC-substructure scale by optimizing FRP schemes to improve progressive-collapse resistance while avoiding an unfavourable strong-beam–weak-column seismic mechanism. Their contribution provides an important mechanism-based design strategy, but it does not assess whole-building retrofit alternatives across different damaged configurations or address masonry construction. Vieira et al. [19] experimentally demonstrated that textile-reinforced mortar (TRM) and near-surface-mounted (NSM) reinforcement can substantially enhance the resistance and deformation capacity of existing

RC frame subassemblies following central-column loss. Their work provided valuable experimental evidence on compressive-arching and tensile-catenary mechanisms, but did not couple progressive-collapse assessment with an intact-building seismic retrofit assessment and did not address masonry construction. For masonry buildings, Kousgaard and Erdogmus [20] investigated an externally applied retrofit system for an existing load-bearing masonry building under several local wall-loss configurations. Their analysis was specifically directed toward progressive-collapse resistance and explicitly excluded seismic loading and the associated retrofit performance; consequently, the interaction between earthquake-oriented strengthening and residual capacity after local damage was not investigated. Their subsequent state-of-the-art review [21] further highlighted the limited guidance and research available for progressive-collapse assessment and rehabilitation of masonry wall buildings, but did not provide a comparative numerical evaluation of alternative seismic retrofit schemes under multiple damaged configurations. More recently, Elkady et al. [22] provided a comprehensive review of progressive collapse, covering collapse mechanisms, standards, analysis procedures, mitigation strategies, structural typologies, and emerging computational approaches. That review confirms the maturity of the broader progressive-collapse field, but does not establish how retrofit alternatives selected from intact-state seismic assessment may be re-ranked when residual load redistribution after local element loss is explicitly considered. The remaining gap is therefore not the separate assessment of seismic performance or progressive-collapse resistance, but their coordinated interpretation across different existing-building typologies. In particular, limited evidence is available on whether alternative retrofit strategies for load-bearing stone masonry retain the same relative effectiveness under seismic loading and under multiple local wall-loss scenarios, or on how such behaviour compares at system level with that of retrofitted RC construction.

Table 1 locates the present contribution against the most closely related studies. The combination of an intact-state seismic assessment, alternative retrofit schemes, and damaged-state checks is not by itself new; the gap addressed here is their coordinated use for masonry alternatives under multiple wall-loss scenarios, alongside a typology-specific RC alternate-load-path screening. The RC case remains illustrative because it contains one column-removal location rather than a multi-location robustness ranking.

Table 1: Literature-gap comparison of retrofit and damaged-state studies.

Study	Structural typology	Intact-state seismic assessment	Retrofit alternatives	Column/wall-loss scenarios	Damaged-state analysis	Multiple-retrofit ranking	Cross-typology interpretation
Scalvenzi et al. [17]	RC frame	Yes; nonlinear static	CFRP shear strengthening	Central and corner column removal	Pushdown analysis	No formal ranking	No
Vieira et al. [19]	RC frame subassemblies	No building-level seismic assessment	TRM and NSM reinforcement	Central-column loss	Experimental subassembly response	Comparison of measures, not building-level ranking	No
Zhang et al. [18]	RC frame substructures	Seismic mechanism constraint; no intact-building assessment	Optimized FRP schemes	Column-loss substructure	Progressive-collapse resistance calculation	Yes, within RC substructures	No
Kousgaard & Erdogmus [20]	Load-bearing masonry	No	Externally applied retrofit system	Several local wall-loss configurations	Damaged-state numerical assessment	No alternative seismic-retrofit ranking	No
Present study	RC frame and stone masonry	Yes; pushover (RC) and modal response-spectrum analysis (masonry)	RC jackets/selected beams; M1–M3 masonry schemes	One RC column; four masonry wall-loss scenarios	RC nonlinear-static alternate-load-path screening; masonry source-study stress/shear-index screening	Qualitative threshold comparison for masonry; RC trials qualitative only	Yes; common decision logic with typology-specific metrics

This study brings these issues together through two numerical case studies. The RC case concerns an irregular six-storey building assessed by pushover analysis, strengthened with RC jackets and selected beam interventions, and reanalysed after removal of a ground-storey column. The masonry case concerns an existing load-bearing stone-masonry building studied in its original condition and with three intervention configurations; four wall-removal scenarios are then used to examine the damaged response. The comparison is not based on direct equivalence between frame and wall response quantities. Instead, it considers four questions that apply to both systems: how much the intact seismic response improves, how demand changes after local loss, whether damage remains localized, and whether the intervention assists the formation of a viable replacement load path.

On this basis, the principal contributions of this study are threefold:

- **A robustness-informed retrofit assessment across two distinct structural typologies.** The study applies a common assessment logic to an existing reinforced-concrete frame and a load-bearing stone-masonry building, while retaining the typology-specific analysis procedures, response quantities, and failure criteria required by each structural system. In both cases, retrofit effectiveness is examined first for the intact seismic configuration and subsequently for a locally damaged configuration, allowing the seismic and robustness objectives to be interpreted within the same decision framework.
- **A comparative assessment of alternative stone-masonry retrofit strategies under multiple local-damage scenarios.** Three materially and mechanically different intervention schemes—shotcrete-based strengthening (M1), grout-injection-based strengthening (M2), and a ring-beam and vertical-prestressing scheme (M3)—are evaluated under four different wall-removal scenarios. Their performance is compared using the source-study in-plane shear screening-index threshold classifications. The available S_{22} output is used only to identify qualitative stress localization, not to establish a complete normal-stress capacity ranking.
- **Evidence that intact-state seismic improvement does not necessarily translate into improved damaged-state robustness.** The comparative results show that retrofit alternatives that improve stiffness and seismic response in the intact structure may develop substantially different levels of residual performance after local element loss. This divergence is particularly evident in the masonry case, where the relative effectiveness of the intervention schemes changes when the reported damaged-state stress and shear checks are considered. The results therefore demonstrate that seismic retrofit selection should not rely exclusively on intact-state performance, but should also include explicit assessment of representative damaged configurations.

Both case studies were modelled and analysed using SAP2000 v27.1.0. The results are used here as comparative evidence within the adopted modelling assumptions. They are not experimental validation and should not be interpreted as a substitute for project-specific assessment based on current provisions, verified material properties, and calibrated structural models.

Accordingly, the study addresses the following research questions:

1. Does the relative seismic ranking of retrofit alternatives change when the same alternatives are assessed after local element loss?
2. Which modelled response features govern damaged-state demand and redistribution in the two structural typologies?
3. Can sensitivity to the damaged-state scenario be used as a criterion for selecting among otherwise effective seismic retrofit alternatives?

2 Structural robustness and progressive collapse

2.1 Terminology and system-level interpretation

Structural robustness concerns the response of a structural system after local damage has occurred. In the terminology adopted here, *progressive collapse* describes the propagation process by which an initial local failure causes one or more subsequent failures, whereas *disproportionate collapse* describes an outcome whose spatial extent or consequences are not commensurate with the initiating event. Robustness is therefore not a separate accidental action and should not be confused with the resistance of an isolated member. It is a system property: a robust structure can tolerate a specified local loss, redistribute the associated actions, and retain an acceptable degree of stability without uncontrolled propagation [6, 7, 23, 9].

This distinction is important because conventional member-by-member verification does not necessarily reveal a system-level weakness. A building may satisfy the prescribed resistance checks for the intact design situation yet remain highly sensitive to the loss of one column, wall pier, transfer member, or connection. Conversely, local damage need not lead to extensive collapse when neighbouring members, floor systems, diaphragms, ties, and connections can mobilize reserve mechanisms. The relevant question is thus not only whether the initially damaged component could have been made stronger, but whether the remaining structure possesses a viable and sufficiently deformable load-transfer route [24, 25, 26].

Historical failures have repeatedly demonstrated the distinction between local damage and collapse propagation. The partial collapse of Ronan Point in 1968 exposed the vulnerability of a large-panel system to the loss of local support, while the 1995 collapse of the Alfred P. Murrah Federal Building illustrated how failure near a transfer system can affect a much larger region. More recent forensic databases confirm that collapse propagation depends on the interaction among the initiating hazard, the location and type of initial failure, structural topology, connection behaviour, and the impact of falling debris on lower levels [9, 27]. These observations support a hazard-informed but system-focused assessment: credible initiating events should be considered where they can be defined, but robustness should also be tested through event-independent local-damage scenarios.

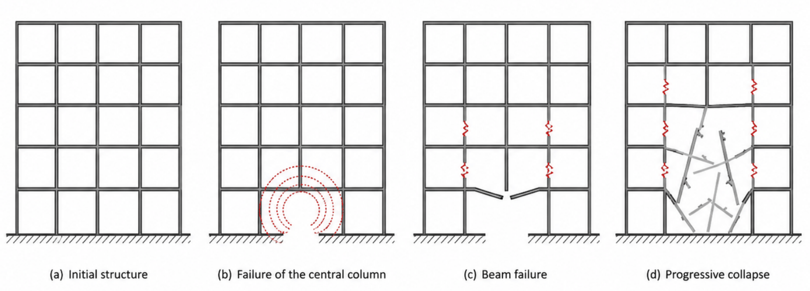

Figure 1: Conceptual distinction between local damage, robust redistribution, and progressive propagation. The initiating event may vary; the robustness assessment concerns the residual structural system and its ability to arrest failure

2.2 Initiation, redistribution, and propagation

A local failure changes both the equilibrium path and the deformation pattern of the structure. Gravity actions previously carried by the removed component must be transferred to the surviving system, often over a very short time. The resulting response may involve flexure, Vierendeel action, compressive arching, membrane action, catenary action, torsion, or interaction with non-structural components. Which mechanism develops depends on the structural typology, the position of the removed element, the available continuity, and the rotational and axial deformation capacity of the connections and surrounding members. Full-scale and subassembly studies of RC structures have shown that load redistribution may differ markedly from that inferred from the intact-state bending-moment diagram, and that connection and anchorage details can govern whether large-deformation mechanisms become available [12, 9, 28].

The rate of damage is equally important. Sudden loss introduces inertia and can produce peak dynamic demand substantially above the corresponding static response. Linear-static procedures account for this behaviour indirectly through load-increase factors, whereas nonlinear static and nonlinear dynamic procedures represent material and geometric nonlinearity with increasing levels of fidelity. The selected procedure should be consistent with the consequence of failure, structural irregularity, expected deformation level, and the uncertainty in the damage scenario [10, 11, 28]. For existing buildings, model uncertainty is often at least as important as analysis sophistication: reinforcement continuity, anchorage, slab participation, masonry bonding, diaphragm connections, and hidden deterioration may determine the residual load path but may not be documented.

A practical robustness investigation therefore proceeds at system level. First, the acceptable extent of damage and the required performance objective are established. Second, one or more critical vertical-load-bearing components are notionally removed, or a physically defined hazard is represented where sufficient information exists. Third, the damaged configuration is analysed under the relevant accidental combination, including geometric nonlinearity and dynamic effects where required. Finally, member forces, deformations, connection demands, stability, and the spatial extent of predicted failure are checked. Because the most adverse location is not always evident in advance, several removal scenarios may be necessary, especially at corners, façades, transfer zones, changes in structural system, and regions with limited redundancy [7, 10, 11].

2.3 Robustness design strategies

The design logic adopted here, following the source investigation, can be organized into three complementary families: specific local resistance, design for an assumed local failure, and indirect integrity provisions. This classification remains useful because it distinguishes measures that prevent the initiating damage from measures that control the structural response after damage.

Specific local resistance and event control. Where a limited number of components can be identified as critical or *key elements*, they may be designed or strengthened to resist a specified accidental action. External measures—such as stand-off distance, access control, protective barriers, or relocation of vulnerable services—can reduce the likelihood or intensity of the initiating event. This approach can be efficient when the threat and the critical components are identifiable, but it cannot provide absolute protection against unforeseen actions exceeding the design assumption. It is therefore commonly combined with system-level measures [25, 7, 24].

Alternate load paths. The alternate-load-path approach assumes that a load-bearing element has become ineffective and verifies that the remaining structure can bridge the damaged region. In frame buildings, the replacement path may mobilize beam flexure, Vierendeel action, compressive arching, or catenary action; in wall buildings, redistribution may depend on lintels, spandrels, orthogonal walls, diaphragms, ring beams, and the integrity of the wall core. The method is attractive because it is largely independent of the initiating hazard, although the assumed removal geometry, application rate, acceptance criteria, and treatment of dynamic amplification materially influence the result [10, 11, 9].

Segmentation and collapse isolation. When an alternative path across a very large span or structural region would be impractical, the objective can change from maintaining complete continuity to arresting propagation at predefined boundaries. Segmentation introduces robust compartment boundaries, discontinuities, fuses, or strengthened interface zones so that failure in one segment does not destabilize the remainder. This strategy highlights an important qualification: continuity and redundancy are generally beneficial, but uncontrolled continuity can also transmit damage and impact forces. Robustness should therefore be judged by the ability to contain consequences, not by continuity alone [23, 26, 9].

Indirect integrity provisions. Prescriptive tying and detailing rules seek to provide a minimum level of structural integrity without explicitly analysing every accidental scenario. Horizontal and vertical ties, dependable anchorage, ductile connections, continuous reinforcement, and adequate rotational capacity improve the likelihood that alternative mechanisms can develop. These rules are particularly useful for ordinary buildings, but they do not demonstrate the performance of an irregular existing structure or verify that the assumed ties can sustain the deformations required after support loss. Direct analysis remains appropriate where consequences are high, load paths are unusual, or the existing details are uncertain [7, 25, 28].

2.4 Implications for seismic retrofit of existing structures

Seismic retrofit and robustness design share several beneficial attributes, including ductility, continuity, energy dissipation, and control of brittle failure. Their objectives are nevertheless not identical. A seismic intervention is normally selected and verified for the intact structure under lateral cyclic demand. A robustness intervention is judged in a damaged configuration in which gravity-load redistribution, large vertical deformation, connection reversal, and membrane or catenary mechanisms can govern. Increasing the strength or stiffness of selected members can therefore improve the seismic response while leaving a weak replacement load path unchanged, or can shift accidental demand to adjacent components that were not strengthened.

For RC frames, robustness depends strongly on the beams, slabs, joints, and reinforcement continuity that bridge a removed column. Column jacketing can be essential for seismic performance and for protecting a key element, but it does not by itself guarantee that the floor system can carry the redistributed gravity loads after the column has been lost. For load-bearing masonry, the corresponding system-level attributes include wall interconnection, diaphragm anchorage, ring-beam continuity, effective lintel and spandrel action, integrity of multi-leaf wall cores, and the capacity to control tensile and in-plane shear demand around openings and removed regions. Measures such as grout injection, shotcrete jackets, prestressing, and ring beams

Robustness objective: limit disproportionate consequences after local damage

Before local damage — event control and specific local resistance. Reduce exposure through stand-off, barriers, and access management; identify and strengthen key elements where a credible accidental action can be specified.

After assumed local damage — direct design. Verify an alternate load path that bridges the removed component, or introduce segmentation and protected boundaries that arrest collapse propagation.

Across all design situations — indirect integrity provisions. Provide horizontal and vertical ties, continuous anchorage, ductile connections, and sufficient rotation and deformation capacity to mobilize reserve mechanisms.

Figure 2: Complementary strategies for limiting progressive and disproportionate collapse. Measures may act before local damage, provide a verified response after notional element loss, or establish a minimum level of integrity through prescriptive detailing.

Table 2: Interpretation of principal robustness strategies for existing buildings.

Strategy	Verification question	Typical retrofit implication
Specific local resistance	Can the identified critical component withstand the prescribed accidental action?	Jacketing, local enlargement, protective barriers, strengthening of transfer elements or supports
Alternate load path	After notional removal, can the remaining structure redistribute gravity actions without violating strength, deformation, or stability limits?	Strengthening of bridging beams, connections, slabs, diaphragms, ring beams, ties, or adjacent wall regions
Segmentation	Can collapse be arrested at defined boundaries without destabilizing adjacent segments?	Strengthened compartment boundaries, deliberate separation, fuses, or protected interface zones
Indirect integrity	Are continuity, anchorage, tie capacity, and ductility sufficient to enable reserve mechanisms?	Continuous reinforcement, improved anchorage, connection upgrading, diaphragm-to-wall ties, confinement and ductile detailing

alter several of these properties simultaneously; their damaged-state effects should therefore be assessed rather than inferred from intact-state modal improvement.

The present study adopts this two-stage interpretation, which follows the robustness framework established in the original RC investigation. Each building is first assessed and strengthened for its intact seismic state. Local element-removal scenarios are then introduced to determine whether the retrofit also improves residual load transfer, limits deformation and overstress, and confines damage to the initially affected region. This sequence follows the central conclusion of the source robustness chapter: the resistance of individual components is not a sufficient proxy for the resistance of the structural system, and retrofit decisions should be checked against both the intact and damaged configurations.

3 Assessment framework

3.1 Seismic performance and robustness as complementary objectives

The seismic assessment objective is to determine whether the intact structure satisfies a prescribed performance level under a selected earthquake action. The robustness objective is to determine whether the damaged structure can sustain the accidental load combination after local loss without disproportionate propagation. These objectives share requirements for strength, deformation capacity, continuity, and redundancy, but emphasize different structural states.

Because the two case studies use different structural systems and analysis procedures, no single scalar seismic or robustness index is imposed. The RC assessment is interpreted using performance-point displacement and base shear, member acceptance states, hinge distributions, and removal-point displacement. Performance-point base shear is retained only as a reported ordinate paired with its target displacement; without the full capacity curves, it is not used to infer initial stiffness or ultimate resistance. The masonry assessment is interpreted using modal periods, control-point response, the source-study in-plane shear threshold classifications, and qualitative localization in the available S_{22} output. The cross-case comparison therefore evaluates the same decision questions—intact-state improvement, residual load transfer, localization of demand, and viability of an alternative load path—while retaining response measures that are physically meaningful for each typology.

The available masonry records do not contain the resistance equations, wall-region dimensions and boundaries, shell-element membership, design strengths and safety factors, or the precise stress/resultant averaging and integration conventions required to reproduce the numerical demand-to-capacity calculations independently. Accordingly, the reported demand-to-capacity ratios (DCRs) are treated exclusively as *source-study screening indices*, not as independently reconstructed capacity checks. Consistent below-/above-threshold classifications are available for the shear index, but not as a complete scenario-by-configuration dataset for the tensile and compressive normal-stress indices. This paper therefore reports the shear threshold matrix but makes no quantitative normal-stress adequacy claim and does not rank M1 against M2 for damaged-state robustness. The nominal separation previously reported between their aggregate shear indices is smaller than plausible variation in masonry properties and intervention effectiveness; without sensitivity analysis it cannot establish that M2 is superior to M1.

3.2 Simulation-driven workflow

Figure 3 documents the study-specific computational sequence used to organize the two case studies and the present cross-case synthesis. It comprises six stages: (1) definition of geometry, materials, loads, and structural information; (2) construction and verification of the finite-element model; (3) baseline seismic assessment; (4) retrofit modelling and reassessment; (5) notional element-removal analysis; and (6) comparative interpretation. Part of the numerical evidence is drawn from the supplied analysis records; the figure describes the analysis-and-synthesis sequence followed in this paper. The digital model is thus used not only as an analysis tool but as a common environment in which intact and damaged configurations are evaluated consistently.

3.3 Standards and interpretation boundaries

The analysis records identify the Greek intervention code (KAN.EPE.), Eurocode 8, ATC-40, Eurocode 6, Eurocode 1, and related guidance as the methodological bases for the adopted checks. This paper interprets

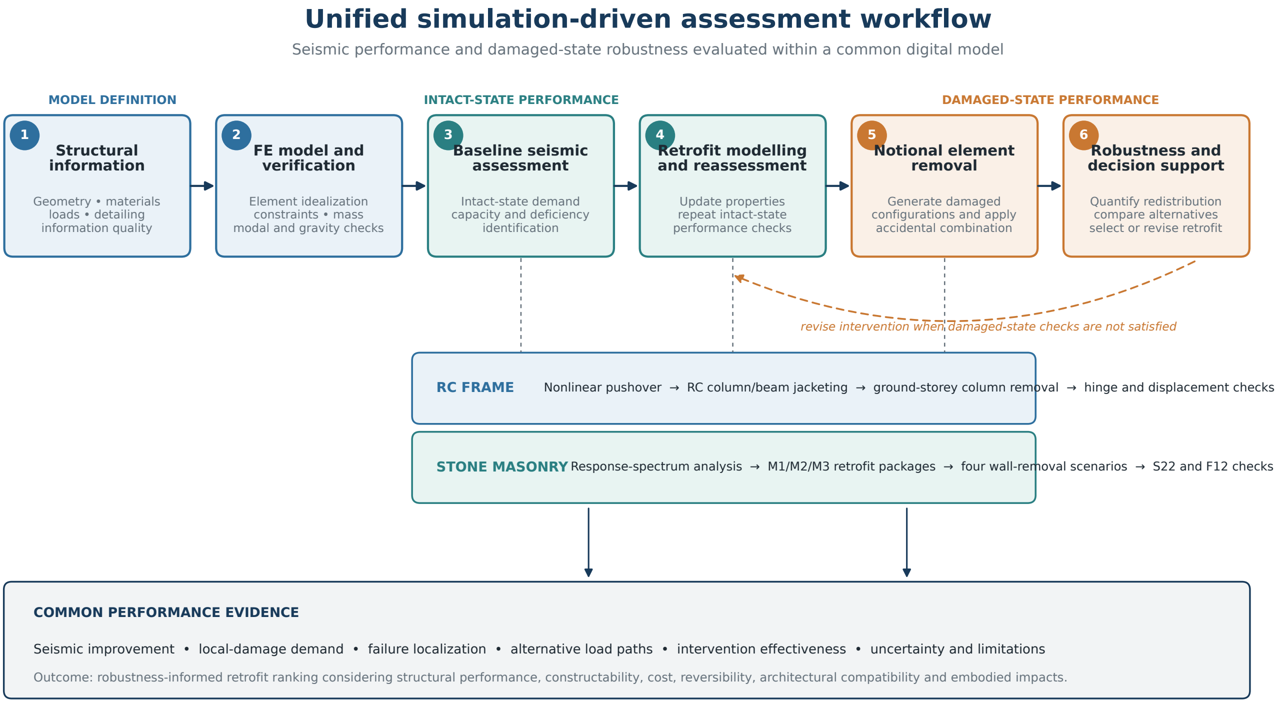

Figure 3: Study-specific simulation workflow used in this paper, linking model definition, intact-state seismic assessment, retrofit modelling, local element removal, damaged-state screening, and cross-case interpretation.

Table 3: Correspondence between the two structural case studies.

Aspect	RC building	Stone-masonry building
Primary system	Six-storey irregular RC frame with wall components	Load-bearing perimeter and internal stone-masonry walls
Baseline seismic method	Nonlinear static pushover	Modal response-spectrum analysis
Retrofit alternatives	RC jacketing of deficient columns and selected beams	M1 shotcrete-based; M2 grout-injection-based; M3 ring beam and vertical prestressing
Local damage	One illustrative ground-storey column removal	Four predefined lower-storey façade wall-removal scenarios
Damaged-state outputs	Plastic-hinge states and removal-point displacement	Direct stress S_{22} and in-plane shear F_{12}
Main decision issue	Development of an acceptable hinge mechanism and bridging action	Improvement of wall strength and redistribution without attributing the combined M3 response to an individual intervention component

the reported results within EN 1990 robustness principles, EN 1991-1-7 accidental actions, and alternate-load-path guidance. UFC 4-023-03 is used only as an interpretive reference and not as the design basis for the reported models. Accordingly, no claim is made that the input values or analyses constitute verification under every currently applicable provision.

Table 4: Principal standards and guidance relevant to the adopted assessment framework.

Document	Role in the study	Interpretation
KAN.EPE.	Existing RC assessment, member modelling, performance checks, retrofit	Basis of the original RC study
EN 1998-1 and EN 1998-3	Seismic action and assessment of existing buildings	Intact-state earthquake assessment
ATC-40 / FEMA 440	Capacity-spectrum and target-displacement concepts	Pushover interpretation
EN 1990	Reliability and robustness principles	General requirement to limit disproportionate damage
EN 1991-1-7	Accidental actions and localized failure strategies	Damaged-state conceptual framework
EN 1996-1-1	Masonry resistance concepts	Material and resistance checks
GSA/UFC guidance	Alternate load path and component removal	Comparative damaged-state interpretation

3.4 Numerical evidence and present-study developments

The present paper reorganizes the supplied evidence within a common intact-/damaged-state framework and distinguishes the model outputs provided in the analysis records from the synthesis, interpretation, and visualizations developed in this paper. Table 5 identifies the provenance of the principal information and the developments introduced here.

All calculations reported in this paper were performed using SAP2000 v27.1.0 [29]. The numerical values must be interpreted within the stated modelling assumptions, not as experimental validation or as a substitute for project-specific verification under current provisions. The present contribution consists of the qualitative cross-scenario comparison, cross-typology framework, and new comparative visualizations identified above.

4 Case study I: reinforced-concrete building

4.1 Structural configuration

The first case represents the stage block of an existing theatre building in Volos, Greece, idealized as structurally separated from adjacent parts by joints. The analysed structure is a six-storey irregular RC building. Floor elevations are approximately 5.12 m, 11.10 m, 13.35 m, 15.62 m, 17.87 m, and 20.37 m. The floor plans, member sizes, reinforcement arrangements, and storey heights vary significantly. Beam-to-beam supports, eccentric beam–column connections, and plan irregularity are present in both principal directions.

The structure was assumed to have been designed according to older Greek provisions, with material and detailing characteristics representative of pre-modern seismic design. The existing concrete was associated with class C12/15 and the reinforcement with S220. For assessment, the mean concrete strength was taken as approximately 18.18 MPa, the reinforcement yield strength as 200 MPa, the concrete modulus as 27 GPa, and the steel modulus as 199 GPa.

4.2 Finite-element model

Beams and columns were represented by three-dimensional frame elements with six degrees of freedom per node. Slabs were not explicitly represented by shell elements; their gravity loads were distributed to beams by tributary areas, while rigid diaphragms were assigned at floor levels. Masonry infills were omitted from

Table 5: Source-derived information versus present-study developments.

Information or output	Evidence supplied in the analysis records	Development in the present paper
Building geometry, member/wall dimensions, materials, supports, loads, and finite-element idealizations	RC model; masonry model	Common terminology and documentation of interpretation boundaries
Retrofit definitions	RC jackets and beam-strengthening trials; masonry configurations M1–M3	Typology-independent intact-/damaged-state comparison logic
Analysis cases and local-loss scenarios	RC pushover and AK22 removal; masonry modal analysis and four wall-removal scenarios	Unified scenario matrix and comparison structure
Raw numerical evidence	Capacity/performance-point data, hinge plots, modal/control-point results, regional S_{22} and F_{12} output, and original screening checks	Consolidation into consistent tables and traceable response measures
Masonry damaged-state screening	Complete qualitative shear-threshold classifications; incomplete normal-stress screening records	Cross-scenario shear-threshold matrix and qualitative S_{22} localization; no reconstructed ratios, normal-stress ranking, or derived statistics
Cross-case interpretation	Not developed across the two source studies	Cross-typology synthesis of modelled demand redistribution and retrofit/load-path compatibility
Figures and visualizations	Original model views, hinge maps, and finite-element output	Redrawn comparison plots, workflow diagrams, and decision framework; source-derived figures are identified in their captions

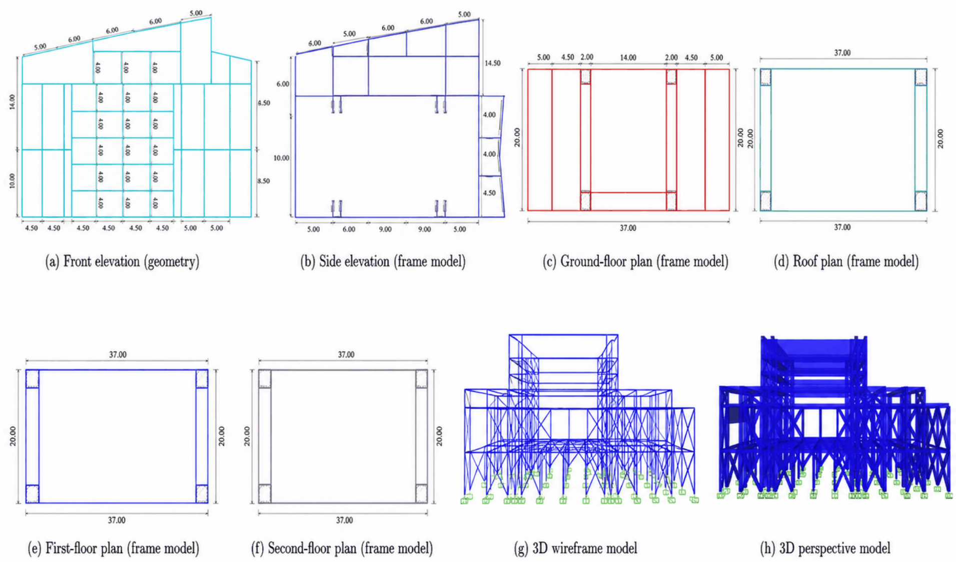

Figure 4: Representative floor plans and three-dimensional finite-element model of the six-storey RC building.

lateral resistance. Wall components were represented using diagonal braces with dimensions derived from the wall length and thickness in accordance with the adopted KAN.EPE. idealization. Base nodes were fixed. Member offsets were used where beams framed eccentrically into columns.

The seismic mass was derived from $G + 0.3Q$. The first mode was translational predominantly in the Y direction, the second predominantly in X, and the third torsional, providing a basic verification of the model's expected behaviour.

Table 6: Principal RC model properties and analysis assumptions.

Parameter	Adopted value or modelling assumption
Concrete / reinforcement	C12/15-equivalent existing concrete; S220 existing reinforcement
Assessment strengths	$f_{cm} \approx 18.18\,\mathrm{MPa}$; $f_y \approx 200\,\mathrm{MPa}$
Elastic moduli	$E_c = 27\,\mathrm{GPa}$; $E_s = 199\,\mathrm{GPa}$
Unit weight	$25\,\mathrm{kN/m^3}$
Slabs	Not explicitly modelled; rigid floor diaphragms and tributary gravity loads
Beams and columns	3D frame elements
Wall components	Equivalent diagonal-brace idealization
Supports	Fixed at foundation level
Mass source	$G + 0.3Q$
Software	SAP2000 v27.1.0

4.3 Loads and seismic action

The permanent area loads used in the source model included $3.0\,\mathrm{kN/m^2}$ for general floor finishes, $1.5\,\mathrm{kN/m^2}$ for stage corridors, and $3.0\,\mathrm{kN/m^2}$ for roofs. Representative wall loads were $3.6\,\mathrm{kN/m^2}$ for heavier walls and $2.1\,\mathrm{kN/m^2}$ for lighter partitions. Imposed loads were $5.0\,\mathrm{kN/m^2}$ for general floors, stairs, and balconies, and $2.0\,\mathrm{kN/m^2}$ for roofs.

The elastic spectrum corresponded to EC8 Type 1, ground type D, with $T_B = 0.20\,\mathrm{s}$, $T_C = 0.80\,\mathrm{s}$, $T_D = 2.50\,\mathrm{s}$, and soil factor $S = 1.35$. The reference peak ground acceleration was $a_{gR} = 0.24g$, and importance class III with $\gamma_I = 1.1$ led to $a_g = 0.264g$.

4.4 Nonlinear static analysis

Moment–curvature response was used to establish yield and ultimate properties. Column hinges were of type P–M2–M3 to represent axial-flexural interaction, while beam hinges were of type M3. Hinges were assigned at member ends. The pushover analysis was displacement-controlled using a roof control node close to the centre of mass and a nominal maximum control displacement of 0.10 m. Gravity loading $G + 0.3Q$ was first applied nonlinearly, followed by lateral loading.

Uniform and modal load patterns were considered in the combinations $\pm X \pm 0.3Y$ and $\pm Y \pm 0.3X$, resulting in 16 pushover cases. The Life-Safety performance level was adopted. Target displacements were determined through the ATC-40 capacity-spectrum procedure.

Table 7: Critical baseline RC pushover cases and reported performance points.

Critical direction / load case	Target displacement (m)	Base shear (kN)
$-X - 0.3Y$ uniform	0.066	19076
$+Y - 0.3X$ uniform	0.011	5817
$-Y + 0.3X$ uniform	−0.011	5646
$+X + 0.3Y$ uniform	−0.067	20374

The baseline analysis identified 15 columns exceeding the Life-Safety chord-rotation limit: AK2, AK12, AK62, AK65, AK66, AK68, AK70, AK72, AK77, AK80, BK12, BK39, BK68, BK72, and BK80. The distribution of deficiencies indicated the need to improve column capacity and to promote a more desirable beam-dominated mechanism.

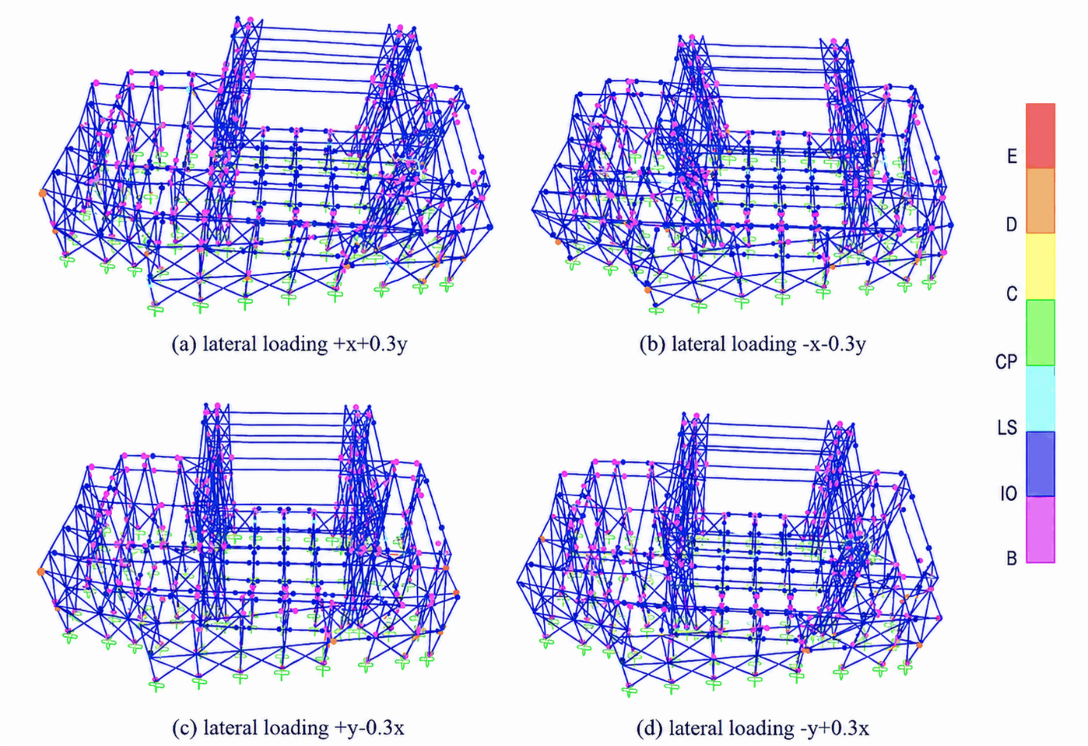

Figure 5: Plastic-hinge states of the existing RC structure at the critical performance points.

4.5 RC retrofit design

Closed RC jackets were applied to deficient columns. Iterative reassessment led to additional strengthening of AK52, DK3, and DK55 so that no column exceeded the selected performance criterion. The final interventions were:

- AK12, BK12, AK62, AK66, AK68, BK68, AK70, AK72, BK72, AK77, AK80, and BK80: 100 mm C30/37 jacket with 8ϕ20 S500 bars;
- AK2 and AK65: 100 mm C30/37 jacket with 8ϕ25 S500 bars;
- BK65 and BK70: 80 mm C30/37 jacket with 8ϕ20 S500 bars;
- DK3 and DK55: 50 mm shotcrete C30/37 jackets with 16ϕ10 and 18ϕ10 S500 bars, respectively; and
- AK52: 50 mm shotcrete C30/37 jacket with 18ϕ10 S500 bars.

After the column retrofit, the tension zones of beams AD16, AD20, and AD24 were strengthened with a 100 mm C30/37 RC layer and 3ϕ16 S500 bars. The final reassessment reported no member exceeding Life Safety.

Table 8: Summary of RC retrofit interventions.

Members	Jacket thickness	Added longitudinal reinforcement	Purpose
AK12, BK12, AK62, AK66, AK68, BK68, AK70, AK72, BK72, AK77, AK80, BK80	100 mm	8ϕ20 S500	Increase axial-flexural capacity and confinement
AK2, AK65	100 mm	8ϕ25 S500	Higher-demand column strengthening
BK65, BK70	80 mm	8ϕ20 S500	Additional column capacity
DK3, DK55	50 mm	16ϕ10, 18ϕ10 S500	Shotcrete strengthening of wall-related members
AK52	50 mm	18ϕ10 S500	Additional iterative retrofit
AD16, AD20, AD24	100 mm layer	3ϕ16 S500	Beam flexural strengthening

4.6 Post-retrofit seismic response

The reported performance points show reduced absolute target displacement in all four critical cases. Performance-point base shear increased in the two Y cases (5817 → 6159 kN and 5646 → 6165 kN) but decreased in the two X cases (20374 → 18538 kN and 19076 → 18507 kN). No hinge exceeded Life Safety. Because the available source material does not provide capacity-curve ordinates, an initial capacity-curve stiffness could not be calculated; performance-point base shear is therefore not used as a proxy for stiffness or resistance.

Table 9: Reported RC performance points before and after retrofit.

Case	d_0 (m)	V_0 (kN)	d_R (m)	V_R (kN)
$+X+0.3Y$	-0.067	20374	-0.062	18538
$-X-0.3Y$	0.066	19076	0.062	18507
$+Y-0.3X$	0.011	5817	0.0096	6159
$-Y+0.3X$	-0.011	5646	-0.0098	6165

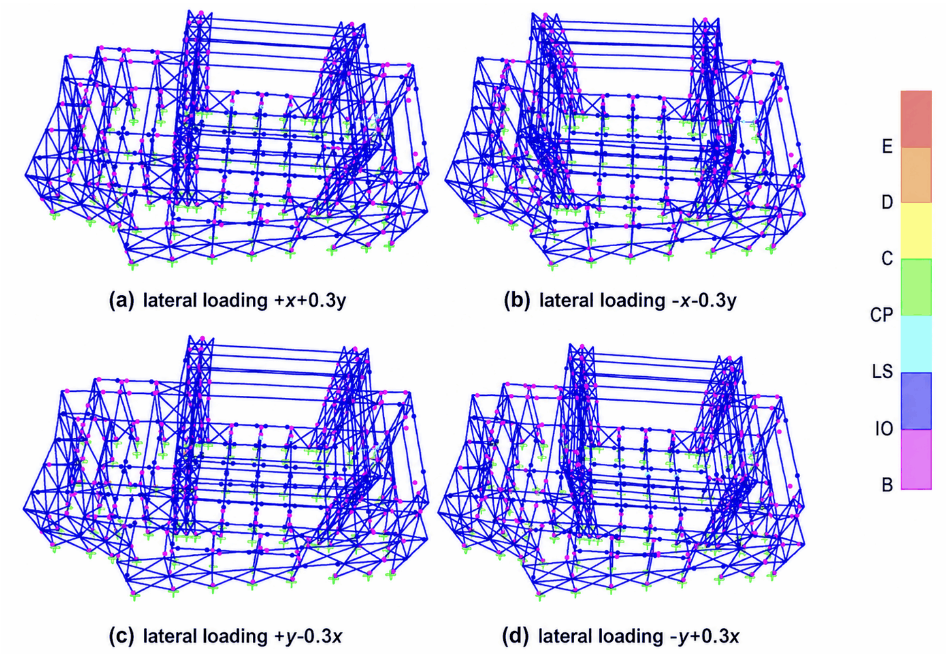

Figure 6: Plastic-hinge states of the retrofitted RC structure at the critical performance points

4.7 Nonlinear-static alternate-load-path screening after column loss

The damaged-state response of the retrofitted RC building was investigated through a nonlinear-static alternate-load-path screening analysis. A ground-storey column, AK22, was removed from the structural model to represent a prescribed local loss of vertical support. The purpose of the analysis was not to reproduce the initiating event itself, but to examine how the remaining structural system redistributed gravity loads after the loss of the selected column.

The retained records do not document a vulnerability scan, tributary-load comparison, accessibility or hazard argument, or corner/interior-column ranking that led to the selection of AK22. It must therefore be treated as an illustrative prescribed ground-storey removal, not as the demonstrated governing column of the building. Its supported physical relevance is limited to its role as a vertical support within the irregular ground-storey frame: once removed, the adjacent beams and joints must bridge the unsupported location and transfer its gravity demand to neighbouring columns. Figure 7 documents its position, but the present paper makes no claim that AK22 has the largest tributary load, the least redundancy, or the most adverse support condition. A systematic robustness assessment would require removal of additional corner, perimeter, and interior columns selected using explicit consequence and redundancy criteria.

The damaged configuration was subjected to the gravity-load combination

$$G + 0.7Q, \tag{1}$$

where G and Q denote permanent and imposed gravity loads, respectively. This combination was adopted in the source numerical analysis and is retained here to preserve consistency among the damaged-state comparisons. It should not, however, be interpreted as a current-code prescription for nonlinear alternate-load-path verification.

The screening was performed in SAP2000 v27.1.0 as a force-controlled nonlinear-static load case. The damaged model started from zero initial conditions with column AK22 already absent, and the gravity load was increased incrementally to its full prescribed value ("Full Load" application control). Material nonlinearity associated with the assigned plastic hinges was included. Geometric nonlinearity was not activated; therefore, P–Δ and large-displacement effects were not represented. Slabs were not explicitly modelled, so slab membrane action was also excluded. Because the column was absent before gravity loading, the analysis did not simulate instantaneous support removal from a preloaded gravity-equilibrium state. Consequently, inertia and dynamic amplification associated with sudden column loss were not captured. The results must therefore be interpreted solely as a nonlinear-static alternate-load-path screening of relative load-redistribution behaviour, not as a dynamic simulation or a code verification of progressive-collapse resistance.

The principal local response quantity was the vertical displacement, U_3, of joint 88, located at the position of the removed column. For comparative purposes, the damaged-state displacement indicator is defined as

$$u_{\text{rem}} = |U_{3,88}|\,, \tag{2}$$

and was examined together with the distribution and severity of plastic-hinge states in the members surrounding the damaged region. These quantities permit a qualitative examination of the reference damaged configuration and the alternative beam-strengthening schemes. Without response values extracted at a common applied load factor, they do not establish a quantitative comparison or ranking and are not formal progressive-collapse acceptance criteria.

The nonlinear solution employed a maximum of 15,000 total steps per stage and 10,000 null steps per stage, with up to 10 constant-stiffness iterations and 40 Newton–Raphson iterations per step. The relative iteration-convergence tolerance was 10^{-4}. Event-to-event stepping was activated with a relative event-lumping tolerance of 0.01. Up to 20 line searches per iteration were permitted, with a relative line-search acceptance tolerance of 0.1. Target-force iteration was limited to 10 iterations per stage with a relative convergence tolerance of 0.01, and the analysis was not allowed to continue following non-convergence. For the reference damaged configuration, application of the prescribed gravity load was completed in 97 analysis steps.

No independent code-based displacement or plastic-rotation acceptance threshold was imposed. Accordingly, the RC nonlinear-static alternate-load-path screening illustrates the response patterns associated with the investigated alternatives but does not quantify their relative effectiveness, rank the trials, or certify compliance with a prescribed progressive-collapse performance limit.

Following the baseline nonlinear-static alternate-load-path screening, three additional strengthening configurations were examined to improve load redistribution around the removed support. In the first configuration, ground-storey beams AD27 and AD28 were strengthened by a 100-mm reinforced-concrete layer with $4\phi25$ S500 longitudinal reinforcement. The second configuration extended the same strengthening to beams AD27, AD28, AD59, and AD263, whereas the third configuration strengthened AD27, AD28, and BD6.

The source investigation reported vertical displacements of joint 88 at analysis step 90, but it did not retain the corresponding load-factor–displacement histories. Because the reference and trial analyses terminated at 97, 98, 99, and 98 steps, respectively, step 90 cannot be treated as a common applied load factor. The reported step-90 values are therefore not used to calculate percentage reductions or to rank the three beam-strengthening alternatives in this paper. A valid quantitative comparison requires re-exporting $U_{3,88}$ versus applied load factor, λ, for the reference configuration and all three trials. The responses should then be compared at $\lambda = 1.0$ if every analysis converged to the full prescribed load; otherwise, they should be compared at the largest load factor reached by all four configurations. Until those histories are available, the three trials remain illustrative and unranked.

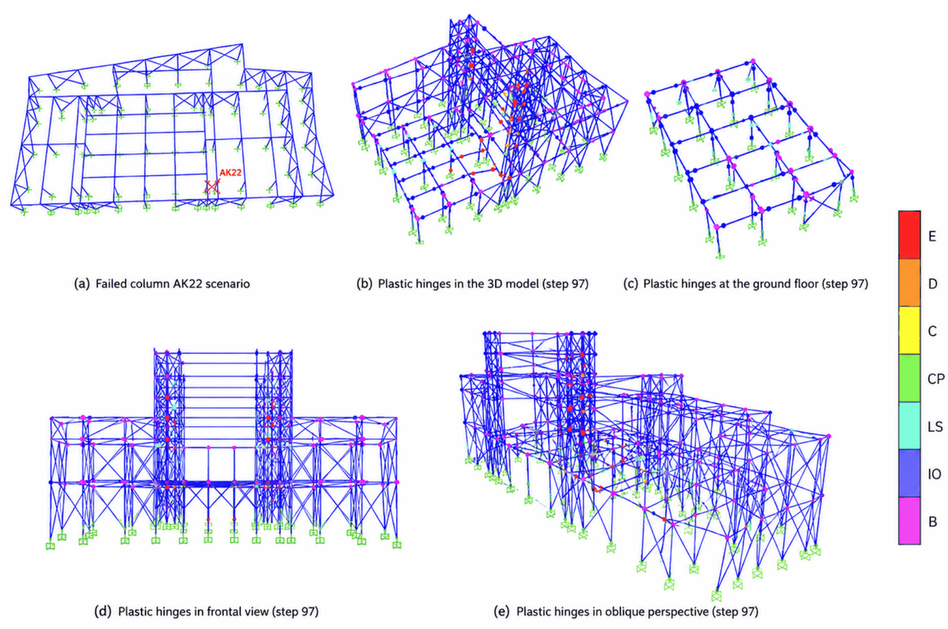

Figure 7: RC column-removal scenario, damaged configuration, alternative load path, and beam-strengthening configurations examined around the removed support

5 Case study II: stone-masonry building

5.1 Structural system and model

The second case comprises perimeter and internal load-bearing stone-masonry walls, floors, a roof, and multiple openings. The masonry is rubble stonework. Shell elements were used to represent walls, with local axes defined so that S_{22} described the critical direct stress and F_{12} the in-plane shear resultant. Floors transferred gravity and seismic actions to the wall system. The model was developed and analysed in SAP2000 v27.1.0 using modal response-spectrum analysis for the intact-state assessment.

Figure 8: Plans, elevations, and three-dimensional shell-element model of the stone-masonry building

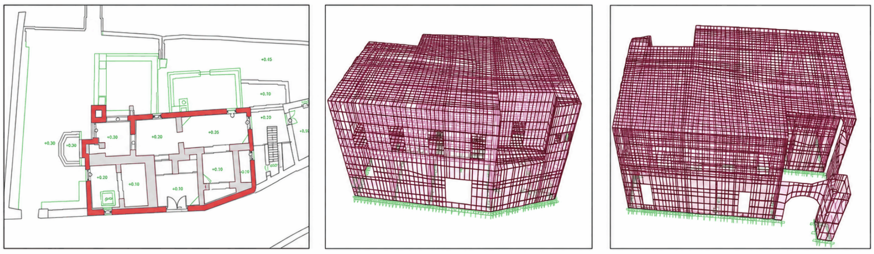

(a) Part of the structure to be modeled and studied. (b) West view of the building under study. (c) East view of the building under study.

Figure 9: Stone-masonry test case and representative masonry FE mesh

5.2 Retrofit configurations

Three intervention packages were assessed: **M1:** mortar-joint repair on the exterior face of perimeter walls, a one-sided shotcrete jacket on the inner face of perimeter walls, and two-sided shotcrete jackets on internal walls; **M2:** mortar-joint repair on both faces of the perimeter walls, grout injection through the wall mass, and two-sided shotcrete jackets on internal walls; and **M3:** mortar-joint repair on both faces of the perimeter walls, an RC ring beam at the top of the first storey, vertical prestressing of perimeter-wall piers, and two-sided shotcrete jackets on internal walls.

M1 improves surface and composite wall capacity but is relatively invasive. M2 improves the internal wall mass while largely preserving external appearance, although execution quality and cost are important. M3 combines repaired joints, a ring beam, vertical prestressing, and internal-wall shotcrete. Because these measures were introduced simultaneously, the model does not isolate the contribution of any individual M3 component to either intact- or damaged-state response.

Table 10: Masonry retrofit configurations and expected structural effects.

ID	Main interventions	Expected benefits	Potential disadvantages
M1	Exterior-face mortar-joint repair; one-sided perimeter shotcrete; two-sided internal-wall shotcrete	Increased compressive, tensile, and shear capacity; improved monolithic action	Added mass; high invasiveness; possible architectural impact
M2	Mortar-joint repair on both faces; grout injection of perimeter walls; internal-wall shotcrete	Homogenized wall core; improved strength and stiffness; preserved facade	Cost, execution sensitivity, uncertain injection completeness
M3	Mortar-joint repair on both faces; RC ring beam; vertical prestressing; internal-wall shotcrete	Combined modification of tying, roof-level continuity, and the initial compression field	Component-specific effects unresolved without an ablation study

5.3 Seismic assessment

Modal analysis was conducted for the existing and three retrofitted models. Effectiveness was evaluated through mode shapes, natural periods, and displacements and rotations at two control points for eight seismic combinations. All interventions shortened the natural periods and reduced control-point translations and rotations. These results support statements concerning modified global stiffness and reduced selected elastic response measures under the adopted response spectrum; without nonlinear capacity analysis, they do not demonstrate increased ultimate load-carrying capacity. Within the single deterministic material-

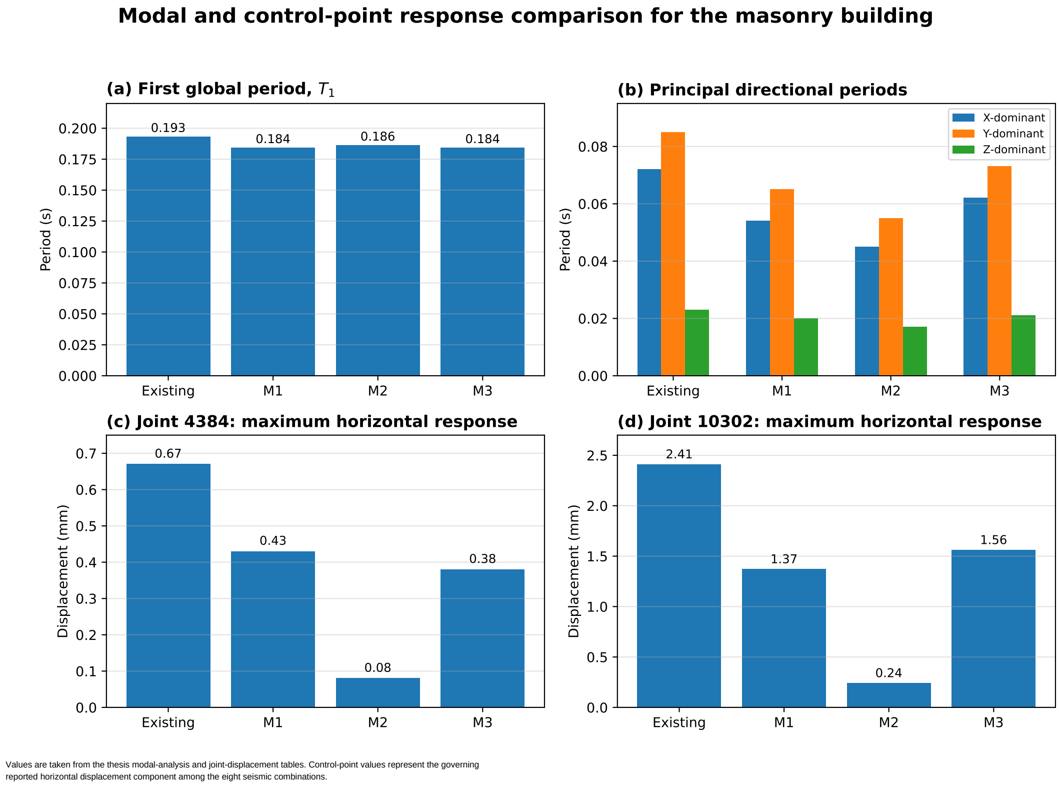

Figure 10: Comparison of fundamental periods and selected control-point responses for the existing, M1, M2, and M3 masonry models.

property set used in the source model, M2 produced the largest reduction in the selected elastic response measures, followed by M1, while the combined M3 configuration was third. This is a nominal ordering of selected intact-state elastic responses, not evidence that M2 is robustly superior to M1 under material and intervention uncertainty. Because the ring beam, prestressing, joint repair, and internal-wall shotcrete were applied together, the M3 ordering also cannot be attributed to any one component.

Table 11: Nominal ordering of selected masonry intact-state responses for the single deterministic parameter set. This is not an uncertainty-informed retrofit ranking.

Reported order	Configuration	Main interpretation
1	M2: mortar-joint repair + grout injection	Largest nominal reduction in selected elastic response measures; robustness of the ordering not tested
2	M1: mortar-joint repair + shotcrete jackets	Second-largest nominal reduction in the selected elastic response measures, with greater intervention
3	M3: combined ring beam + vertical prestressing scheme	Reduced selected elastic response measures relative to the existing model; component-specific cause not isolated

5.4 Local wall-removal scenarios and acceptance criteria

Four accidental scenarios were introduced by removing lower-storey load-bearing wall segments at different façade locations. The accidental gravity combination was then applied to the damaged model. Each scenario was analysed for the existing building and for M1–M3. The source study defined a direct-stress index from the top and bottom S_{22} values and the corresponding masonry resistance, together with a shear index based on F_{12} demand and in-plane shear resistance. These DCR-type quantities are described here only as source-study screening indices. The retained records support a complete qualitative threshold matrix only for the shear index; the normal-stress values, governing regions, and threshold classifications are incomplete. Because the masonry walls were represented by equivalent-continuum shells, the retained results provide only damaged-state screening evidence under the adopted continuum model. They do not simulate discrete cracking, mortar-joint opening, rocking, crushing, interface debonding, or collapse propagation. The supplied source records identify the scenario geometry but do not retain the complete region boundaries, element assignments, resistance parameters, or region-by-region force/stress tables required to reconstruct the indices independently.

The documented selection procedure for S1–S4 is incomplete. In particular, the records do not provide a preliminary ranking based on tributary gravity load, opening density, diaphragm support, wall redundancy, hazard exposure, or expected consequence. The scenarios must therefore be regarded as a predefined comparative sample rather than a verified set of governing removals. Table 12 separates the documented removal geometry from the physical interpretation adopted in the present paper. The interpretations describe the load-path features exercised by each geometry; they are not evidence that these features formed the scenario-selection criteria.

Table 12: Documented masonry removal geometry and present-paper physical interpretation.

Scenario	Documented removal geometry	Load-path feature sampled	Selection-status qualification
S1	East façade: 5.55-m-long, 0.55-m-thick segment	Extended interruption of one façade wall line; redistribution along the remaining east wall and around adjacent openings	Illustrative single-façade removal; tributary load and redundancy ranking not retained
S2	East façade: 2.45 m × 0.50 m; south façade: 2.40 m × 0.50 m	Coupled interruption of two orthogonal façades; tests loss of return-wall continuity and two-direction load transfer	Illustrative orthogonal-façade removal; original corner/support rationale not retained
S3	West façade: 2.00 m × 0.70 m; south façade: 4.15 m × 0.50 m	Asymmetric two-façade interruption with unequal lengths and wall thicknesses; tests redistribution across different wall lines and opening layouts	Illustrative location/geometry variant; no documented worst-case screening
S4	West façade: 1.65 m × 0.70 m; north façade: 3.10 m × 0.60 m	Alternative asymmetric orthogonal-façade interruption; tests sensitivity to façade location, segment length, and thickness	Illustrative location/geometry variant; selected for future ablation because the retained shear classifications distinguish M3 from M1/M2, not because it is proven globally governing

5.5 Source-study damaged-state screening-index outcomes

The available records consistently retain whether the regional in-plane shear indices were below or above the threshold adopted in the source study. Because the underlying resistance inputs, wall-region definitions, element assignments, and force-resultant integration rules are unavailable, the numerical ratios are not reproduced here. Table 13 reports only these shear-threshold classifications. They are not an independent recalculation and should be interpreted solely as source-study screening-index outcomes within the equivalent-continuum model. An equivalent table is not provided for normal stress because the governing tensile and compressive indices, critical regions, and threshold outcomes are not available for every

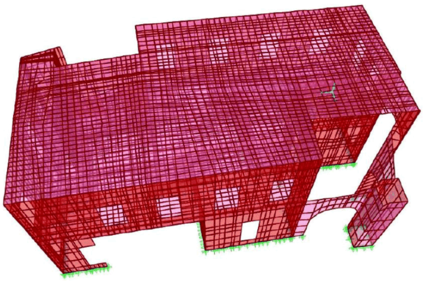

(a) Removal of a 5.55 m-long, 0.55 m-thick masonry segment from the east façade of the building.

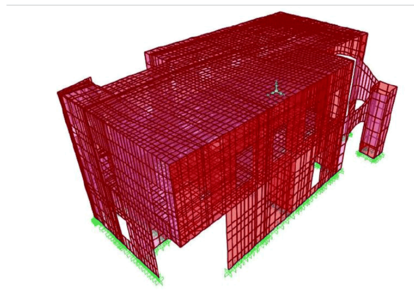

(b) Removal of a 2.45 m-long, 0.50 m-thick masonry segment from the east façade and a 2.40 m-long, 0.50 m-thick masonry segment from the south façade.

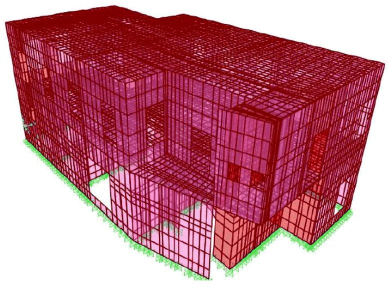

(c) Removal of a 2.00 m-long, 0.70 m-thick masonry segment from the west façade, together with a 4.15 m-long, 0.50 m-thick masonry segment from the south façade.

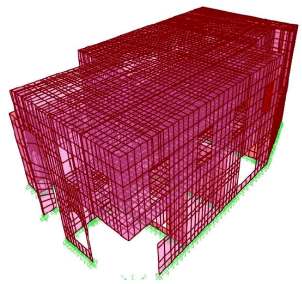

(d) Removal of a 1.65 m-long, 0.70 m-thick masonry segment from the west façade, together with a 3.10 m-long, 0.60 m-thick masonry segment from the north façade.

Figure 11: Four masonry wall-removal geometries, with the removed regions highlighted in the finite-element views. Redrawn from the source investigation; the available records do not document a systematic worst-case selection procedure.

configuration and scenario.

Table 13: Reported position of the source-study in-plane shear screening indices relative to the adopted threshold under the four wall-removal scenarios.

Configuration	Scenario 1	Scenario 2	Scenario 3	Scenario 4
Existing structure	Above threshold	Below threshold	Below threshold	Above threshold
M1	Below threshold	Below threshold	Below threshold	Below threshold
M2	Below threshold	Below threshold	Below threshold	Below threshold
M3	Above threshold	Above threshold	Above threshold	Above threshold

The reported classifications indicate that damage location affected the existing model. M1 and M2 remained below the source-study shear DCR threshold in all four examined scenarios, whereas M3 exceeded that threshold in every scenario. The available evidence does not distinguish quantitatively between M1 and M2; they are therefore treated as unranked for damaged-state shear performance. It also does not identify whether the M3 outcome is attributable to the ring beam, prestressing, internal-wall shotcrete, or their interaction. The available S_{22} output shows where direct-stress concentrations occur in selected model views, but it does not support a complete comparison of tensile or compressive adequacy among Existing, M1, M2, and M3 across the four scenarios.

6 Cross-case mechanism synthesis

The detailed results are reported with the individual case studies in Sections 4 and 5. The synthesis here addresses why intact- and damaged-state response can lead to different retrofit-selection implications, rather than repeating the scenario values. No quantitative ranking of the RC beam-strengthening trials is inferred.

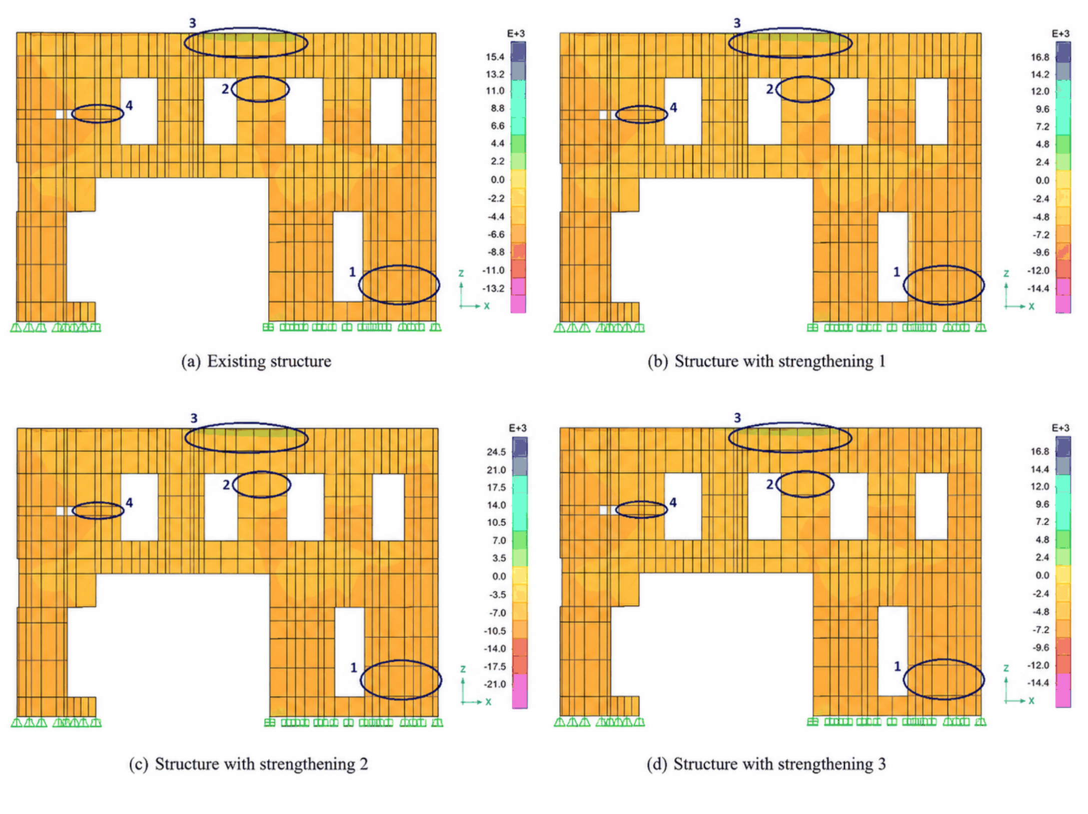

Figure 12: Representative finite-element S_{22} output for a selected masonry wall-removal scenario. Exported from the SAP2000 v27.1.0 model. The figure illustrates stress localization only; no quantitative normal-stress adequacy ranking is inferred.

6.1 Why damaged-state response may alter retrofit selection

Intact-state seismic assessment is governed mainly by lateral stiffness, strength, modal characteristics, and deformation capacity while the original vertical-load system remains available. Element removal changes the topology of that system. The relevant question becomes whether the surviving members can bridge the lost support and transfer gravity load into adjacent bays, walls, diaphragms, or foundations. A retrofit can therefore improve the intact response without strengthening the particular components or connections that become critical after local loss.

In the RC case, column jacketing addresses the observed seismic member deficiencies, but the removed column cannot contribute to the damaged-state load path. Redistribution must instead occur through the beams, joints, and any participating floor system spanning the unsupported region. This observation motivates the beam-strengthening trials but does not determine their relative effectiveness because their responses have not been compared at a common load factor. In the masonry case, M1 and M2 act over substantial wall regions and improve the material participating in redistribution, whereas the combined M3 configuration changes tying, restraint, and the initial stress field without consistently reducing the local in-plane shear demand identified around the removed regions. These observations explain why damaged-state assessment can alter retrofit selection; they do not isolate the causal contribution of any single M3 component.

6.2 Activated replacement load paths

Table 14 compares the replacement paths examined in the two typologies. The common principle is compatibility between the intervention and the post-damage load path, not equivalence of the response quantities used for frames and walls.

Table 14: Mechanism-based cross-typology synthesis.

Issue	RC building	Masonry building
Baseline weakness	Column chord-rotation exceedances and undesirable hinge concentration	Low tensile/shear resistance and stress concentration around openings and removed walls
Intact-state mechanism	Member strengthening, confinement, and control of the hinge sequence	Modification of wall stiffness, strength, and global connectivity
Replacement path after local loss	Beam/joint bridging and plastic redistribution above the removed column; slab action was not modelled	Redistribution through adjacent and orthogonal walls, wall regions around openings, diaphragms, and ring-beam ties
Compatibility requirement	Strengthen the members and connections that must span the unsupported bay	Improve the wall regions and connections that receive diverted normal and shear demand
Mechanism not established by the model	Dynamic amplification, geometric nonlinearity, catenary action, and slab membrane action	Discrete cracking, joint opening, rocking, crushing, debonding, and collapse propagation
Evidence boundary	One illustrative column-removal screening; no multi-location RC ranking	Four wall-removal scenarios under deterministic properties and an equivalent-continuum model

7 Discussion

7.1 Mechanistic interpretation

The change in ranking follows from a change in the governing structural task. Under earthquake loading, the intact system benefits from added stiffness, strength, confinement, and improved connectivity. After local loss, those attributes are useful only if they lie on the replacement load path. In a frame, this path must cross the unsupported bay through beams, joints, reinforcement continuity, and potentially the slab. In a wall building, diverted load must pass through adjacent wall regions, orthogonal walls, spandrels, diaphragms, and ties around the opening created by the removal. Retrofit effectiveness is therefore controlled by load-path compatibility rather than by the nominal resistance added to the removed or strengthened component.

This interpretation is consistent with the mechanisms identified in the literature. Scalvenzi et al. [17] showed that strengthening directed at brittle RC mechanisms can benefit both seismic and damaged-state response, while Zhang et al. [18] showed that progressive-collapse strengthening must remain compatible with the desired seismic hierarchy. The arching and catenary mechanisms observed experimentally by Vieira et al. [19] illustrate the large-deformation frame response that a sufficiently continuous system may mobilize. For masonry, Kousgaard and Erdogmus [20] similarly emphasized residual wall-system continuity after local loss. The present synthesis extends this mechanism-based view by comparing the source-study screening-index threshold classifications across several masonry retrofit configurations and removal locations after intact-state seismic assessment.

The masonry comparison also illustrates why causality must be assigned cautiously. M1 and M2 modify broad portions of the wall system, whereas M3 simultaneously introduces a ring beam, vertical prestressing, repaired joints, and internal-wall shotcrete. The observed M3 threshold outcome is therefore associated only with the combined configuration and cannot be attributed to the ring beam, prestressing, or their interaction.

The appropriate mechanistic test is a controlled M3 ablation study. Starting from an identical repaired-joint and internal-wall-shotcrete baseline, three variants should be analysed: M3a with the ring beam only, M3b with vertical prestressing only, and M3c with both the ring beam and prestressing. At minimum, all three variants should be evaluated for wall-removal Scenario 4 using identical geometry, mesh, material properties, boundary conditions, accidental load combination, solver settings, and regional result-extraction rules. Comparisons should include the governing source-study shear screening index, its critical region, the corresponding F_{12} distribution, and changes in the initial compression field. The same analysis should also be repeated for the intact state so that any damaged-state effect can be distinguished from the stiffness and stress changes introduced before wall removal. These analyses were not performed here because the complete editable model and reproducible regional resistance/extraction inputs were unavailable.

7.2 Required masonry sensitivity analysis

The distinction between M1 and M2 cannot be considered robust until material and intervention uncertainty is propagated through the intact and damaged models. A minimum deterministic one-at-a-time campaign should use the parameter variations in Table 15. The full set of four wall-removal scenarios should be rerun where possible; Scenario 4 is the minimum case because it is the most informative location for comparing the retrofit configurations. In addition to the one-at-a-time cases, combined lower- and upper-bound parameter sets should be analysed to identify interaction effects and possible changes in the critical wall region.

Table 15: Minimum deterministic sensitivity-analysis plan for the masonry models. Multipliers are applied to the documented baseline inputs.

Parameter	Low case	High case	Required application and outputs
Masonry elastic modulus, E_m	$0.80E_m$	$1.20E_m$	Existing and M1–M3; periods, control-point responses, S_{22} localization, and shear-index threshold outcome
Masonry tensile strength, f_t	$0.80f_t$	$1.20f_t$	Existing and M1–M3; governing tensile region and normal-stress screening index where reproducible
Masonry shear resistance	$0.80V_{Rd}$	$1.20V_{Rd}$	Existing and M1–M3; governing shear index, threshold status, and critical region
Grout effectiveness, η_g	$0.80\eta_g$	$1.20\eta_g$	M2; vary the documented grout-induced stiffness and strength gains consistently
Effective prestressing force, P_0	$0.80P_0$	$1.20P_0$	M3 and future M3b/M3c variants; initial compression field, governing shear index, and critical region

For each case, the same geometry, mesh, boundary conditions, load combinations, solver settings, and result-extraction regions must be retained. M2 should be judged superior to M1 only if its advantage persists across the parameter ranges and the identity of the governing region is stable. The present records do not permit this campaign to be executed: the editable models, complete resistance inputs, grout-property mapping, prestress definition, and regional extraction data are unavailable. Accordingly, this paper reports the deterministic intact-state ordering but treats M1 and M2 as indistinguishable in the damaged-state shear screening.

7.3 Scope of generalization

Three conclusions can be transferred beyond the specific buildings: intact- and damaged-state assessments test different load paths; removal-location sensitivity is a useful selection attribute; and retrofit decisions should consider whether source-study screening indices remain below their adopted thresholds across credible damage locations. These are procedural conclusions rather than universal preferences for a material or strengthening technique.

The reported outcomes remain case-specific. The RC evidence covers one removed column and a nonlinear-static model without sudden removal, geometric nonlinearity, or slab participation. It supports the importance of beam and connection bridging but not a general ranking of RC retrofit schemes or removal locations. The masonry evidence covers four removals but uses deterministic material properties and equivalent-continuum shell stresses. It supports qualitative comparative screening within that model, not predictions of discrete cracking, rocking, debonding, or collapse propagation. Consequently, the recorded M1–M3 outcomes should not be generalized to other masonry buildings without sensitivity analysis, verified material data, and explicit consideration of their wall and diaphragm topology.

7.4 Digital-engineering implications

The digital-engineering contribution can be implemented as a version-controlled analysis pipeline rather than as a sequence of manually interpreted model views. The proposed operational chain is

$$\begin{aligned}\text{model manifest} &\rightarrow \text{scenario generation} \rightarrow \text{SAP2000 execution/export}\\ &\rightarrow \text{validated CSV records} \rightarrow \text{screening-index calculation}\\ &\rightarrow \text{aggregation/ranking} \rightarrow \text{plots and report tables.}\end{aligned}$$

Each run begins from an immutable model manifest containing the model identifier, file checksum, SAP2000 version, unit system, material-set identifier, retrofit configuration, analysis-case definitions, and solver settings. A scenario generator then creates intact and damaged variants from explicit component lists rather than from manually renamed files. For example, an RC scenario records the removed frame-object identifier, while a masonry scenario records every removed shell identifier and its assigned wall region. The generated model receives a unique `run_id` linking the input manifest, solver output, and all subsequent tables.

SAP2000 exports should be converted without manual transcription to a long-format result table. Required exports include load factor and monitored displacement for the RC alternate-load-path cases; base shear, control displacement, and hinge state for pushover cases; and shell identifier, region identifier, S_{22} face values, and F_{12} for masonry cases. Table 16 defines the minimum archival data contract. Separate files may be used, but the identifiers and units must remain consistent so that every derived value can be traced to a model, scenario, analysis case, increment, and finite-element entity.

Table 16: Minimum machine-readable data contract for the proposed simulation and post-processing pipeline.

Artifact	Required fields	Function and validation rule
Model manifest	`model_id`, checksum, `sap_version`, units, material set, retrofit ID, solver settings	Identifies the exact input model; execution stops if the checksum, software version, or unit declaration is missing
Scenario manifest	`scenario_id`, parent model, state, removed-object IDs, region map, load-case IDs	Generates intact/damaged variants and preserves the component-level definition of every removal
Raw result table	`run_id`, case, step, load factor, entity/region ID, response name, value, unit	Stores unrounded SAP2000 exports in long format; duplicate keys, unknown entities, and mixed units are rejected
Resistance/method table	`method_id`, equation version, resistance inputs, safety factors, averaging/integration rule, threshold	Makes every screening-index definition explicit; no DCR is calculated when an input or rule is absent
Derived result table	`run_id`, scenario, retrofit, metric, demand, resistance, index, critical entity/region, status	Records traceable calculated metrics and the location controlling each result
Scenario summary	scenario, retrofit, common load level, governing index, pass count, uncertainty range, rank eligibility	Aggregates only comparable runs; ranking is suppressed when load levels differ, inputs are incomplete, or uncertainty ranges overlap

The corresponding processing logic is intentionally solver-independent after export:

1: **READ** the model and scenario manifests; verify checksums, units, object IDs, and the declared SAP2000 version.
2: **GENERATE** each retrofit–damage combination from its parent model and assign a unique `run_id`.
3: **RUN/EXPORT** the specified SAP2000 cases and write unrounded response records to the raw-result schema.
4: **VALIDATE** convergence, expected entities, region membership, units, and common comparison load levels.
5: **CALCULATE** each metric using the versioned `method_id`; retain demand, resistance, critical entity/region, and threshold status. If the method definition is incomplete, return `not_reproducible` rather than an estimated DCR.
6: **AGGREGATE** by scenario and retrofit, including governing values, threshold counts, and sensitivity ranges; compare RC trials only at $\lambda = 1.0$ or the largest common converged load factor.
7: **RANK** only eligible alternatives under declared decision rules, and **PLOT** capacity curves, hinge counts, response histories, regional maps, and scenario summaries directly from the derived tables.

This structure provides an audit trail from a plotted point or reported classification back to the exact solver record and model version. It also supports batch sensitivity analysis, uncertainty propagation, optimization, and eventual linkage to inspection or digital-twin data. It is presented here as the reproducibility specification for a complete computational campaign; the incomplete regional resistance definitions and element-level exports identified in the Data availability statement prevent execution of the full pipeline for the supplied masonry results.

7.5 Practical retrofit-selection framework

This subsection moves beyond the study-specific workflow in Fig. 3. The figure below is a generalized engineering decision framework for future projects: it adds formal information-quality review, hazard- and consequence-based scenario selection, uncertainty-aware comparison, multi-criteria decision-making, and reproducibility requirements. These broader activities are outside the supplied scope of the two case studies and should not be read as a second depiction of the analyses reported here. For existing buildings exposed to both seismic and accidental actions, the following sequence is recommended:

1. establish structural information quality and model uncertainty;
2. assess the intact structure under the governing seismic actions;
3. design preliminary interventions for deficient mechanisms;
4. repeat the seismic assessment and verify that stiffness changes have not created new concentrations;
5. define credible local-damage scenarios based on accessibility, hazard exposure, and structural consequence;
6. evaluate damaged-state redistribution using appropriate static and, where necessary, nonlinear dynamic procedures;
7. rank alternatives using structural performance, intervention cost, embodied impacts, reversibility, and architectural compatibility; and
8. document assumptions and make analysis data available for independent verification.

7.6 Limitations

The principal limitations are:

- the RC and masonry cases used different intact-state analysis methods and therefore require normalized rather than direct raw-response comparison;
- the RC column-loss investigation was a nonlinear-static alternate-load-path screening initiated from zero conditions with the column already absent; sudden removal from gravity equilibrium, inertia, dynamic amplification, P–Δ, and large-displacement effects were not simulated;
- the $U_{3,88}$–load-factor histories were not retained, so the RC beam-strengthening trials cannot be compared or ranked at a common applied load factor;
- AK22 was an illustrative prescribed removal; the available records do not document a systematic corner/perimeter/interior-column screening or demonstrate that it is the governing RC location;
- slabs were not explicitly modelled in the RC system, so slab membrane action was excluded from the screening;

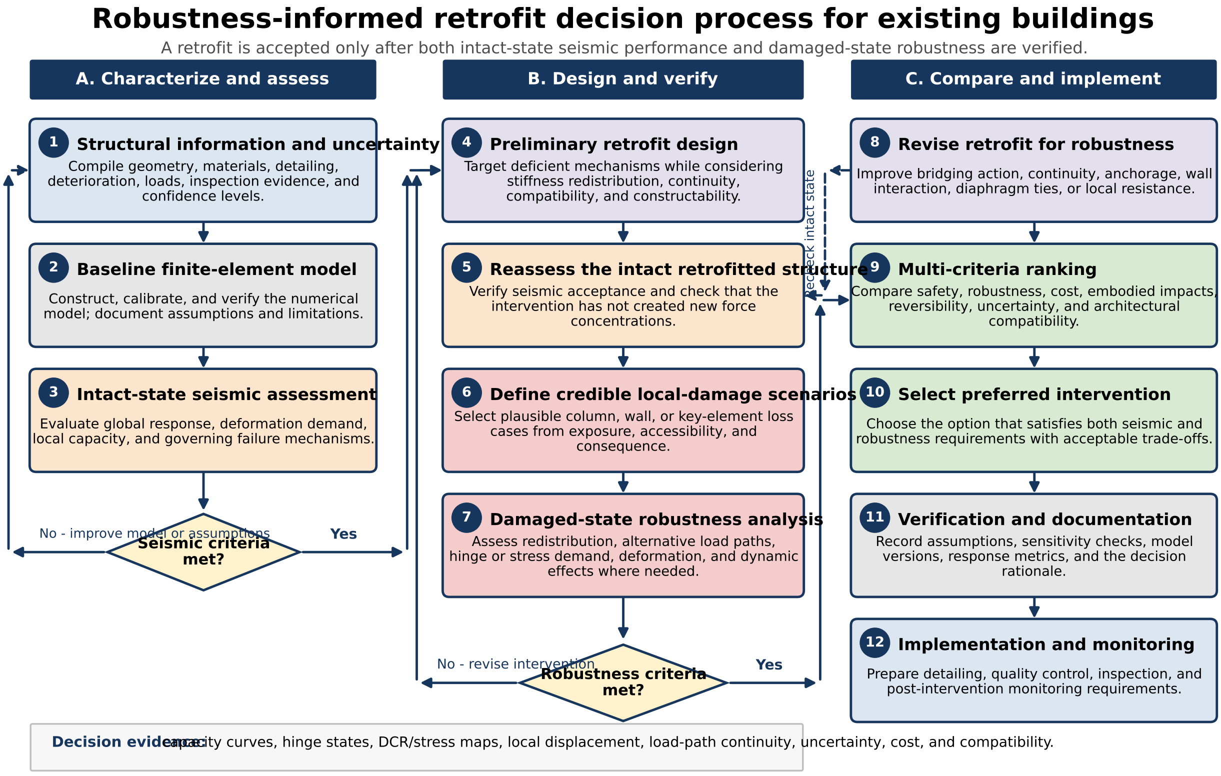

Figure 13: Generalized robustness-informed engineering decision framework for future retrofit projects. Unlike Fig. 3, this figure presents prospective project-level guidance rather than the study-specific computational sequence.

- masonry was represented through an equivalent continuum shell model and did not explicitly simulate joint opening, rocking, cracking, crushing, or interface debonding;
- the retained normal-stress records do not provide a complete scenario-by-configuration set of governing tensile/compressive indices, critical regions, and threshold classifications;
- no M3 ablation models were available, so the effects of the ring beam, vertical prestressing, and their interaction cannot be separated;
- sensitivity to E_m, masonry tensile strength, shear resistance, grout effectiveness, and prestressing force was not evaluated; consequently, the nominal M1–M2 ordering is not uncertainty-informed;
- the physical selection rationale for masonry Scenarios 1–4 was not retained, so the scenario set cannot be claimed to be exhaustive or systematically governing;
- the present masonry comparison is based on the scenario definitions and governing regional results retained from the source investigation; complete element-level result exports from the original model files were not available for this synthesis; and
- no experimental validation was available.

These limitations mean that the results are best interpreted as comparative evidence and as a basis for a renewed numerical campaign, rather than as final design certification.

8 Conclusions

A unified simulation-driven framework was developed to compare seismic retrofit and progressive-collapse robustness in an existing RC building and an existing stone-masonry building. The following conclusions are supported by the source analyses:

1. The baseline RC pushover assessment identified 15 columns exceeding the Life-Safety chord-rotation criterion. Iterative RC jacketing and selective beam strengthening removed the reported exceedances and reduced the number of components entering advanced inelastic states.
2. Global performance-point values alone did not fully characterize retrofit success. The mixed changes in performance-point base shear do not establish a global stiffness increase or greater ultimate resistance

because the complete capacity-curve ordinates were unavailable. Capacity curves must be interpreted together with target displacements, hinge distributions, and member acceptance states.

3. Under ground-storey column loss, the nonlinear-static screening examined beam strengthening around the removed support and the associated hinge patterns. The trials remain illustrative and unranked. A quantitative comparison requires re-exported $U_{3,88}$–load-factor histories evaluated at $\lambda = 1.0$, if reached by every analysis, or at the largest common converged load factor.
4. All three masonry retrofit configurations modified the modal properties and reduced the selected elastic response measures under the adopted response spectrum. For the single deterministic parameter set, M2 produced the largest reduction, followed by M1 and M3. This nominal ordering was not tested under material or intervention uncertainty, should not be interpreted as a robust preference for M2 over M1, and does not establish increased ultimate load-carrying capacity.
5. Under four local wall-removal scenarios, M1 and M2 remained below the source-study shear DCR threshold in every examined scenario, whereas M3 exceeded that threshold in every scenario. M1 and M2 are unranked because the available evidence and missing sensitivity analysis do not establish a robust difference. These source-study screening-index outcomes apply only to the adopted equivalent-continuum model and are not a simulation of masonry progressive collapse.
6. The best seismic intervention is not necessarily the best robustness intervention. Retrofit design should explicitly evaluate the damaged structural state and the availability of alternative load paths.
7. For RC frames, robustness-oriented retrofit should prioritize continuity, beam deformation capacity, and connection/load-path performance. For masonry, it should prioritize wall-core integrity, diaphragm and orthogonal-wall connectivity, and control of tensile and shear demand around openings and removed regions.

Future work should extend the SAP2000 v27.1.0 models to include explicit slab participation and rerun the governing RC case from a gravity-equilibrated intact state followed by sudden column removal, with geometric nonlinearity and nonlinear dynamic analysis. For masonry, priority should be given to the Scenario 4 M3 ablation defined above and to the ±20% sensitivity campaign in Table 15. M3a should include the ring beam only, M3b prestressing only, and M3c both components, using an otherwise identical retrofit baseline and reproducible regional result extraction. Future analyses should also use nonlinear masonry constitutive models, quantify epistemic and aleatory uncertainty, and optimize retrofit alternatives with respect to safety, cost, embodied carbon, reversibility, and heritage constraints.

Data availability

The numerical inputs required to reproduce the regional masonry resistance checks independently—including wall-region definitions, element membership, strength and safety-factor inputs, grout-property mapping, prestress definition, and the stress/resultant extraction rules—are not available in a complete archival dataset. Accordingly, the masonry DCRs are treated only as source-study screening indices. The paper reports the retained below-/above-threshold shear classifications but presents no numerical DCR values or derived cross-scenario statistics. Because complete tensile/compressive indices, critical regions, threshold outcomes, and parameterized model inputs are unavailable, no quantitative normal-stress table or uncertainty analysis is reported. The SAP2000 v27.1.0 model files and complete element-level exports are not included with this article. A renewed archival package should implement the manifests, long-format result records, versioned calculation rules, and traceability fields specified in Table 16.

CRediT authorship contribution statement

Chara Ch. Mitropoulou: Conceptualization, Methodology, Supervision, Project administration, Writing–review and editing. **Matilda Kouramanou:** Investigation, Software, Formal analysis, Data curation, Visualization, Writing–original draft. **Maria Dagalaki:** Investigation, Software, Formal analysis, Data curation, Visualization, Writing–original draft. **Maria Gkara:** Investigation, Writing–review and editing.

Declaration of competing interest

The authors declare that they have no known competing financial interests or personal relationships that could have appeared to influence the work reported in this paper.

Funding

The ADAPT4CE project, "Adaptive digital systems for sustainable construction and material management in the circular economy" (No. 101182768), supported the cross-case synthesis, reproducibility framework, visualization, and manuscript preparation reported in this article. The SAP2000 analyses were outside the scope of this funding. ADAPT4CE is funded under the Marie Skłodowska-Curie Actions (MSCA) Research and Innovation Staff Exchange, HORIZON-MSCA-2023-SE. Views and opinions are those of the authors only and do not necessarily reflect those of the European Union or the European Commission.

Acknowledgements

The authors acknowledge the National Technical University of Athens and the Institute of Structural Analysis and Antiseismic Research for academic, computational, and technical support associated with the structural modelling and manuscript synthesis.

Declaration of generative AI and AI-assisted technologies in the writing process

During preparation of this manuscript, the authors used an AI-assisted language and document-development tool to support restructuring, language editing, LaTeX preparation, and synthesis of the two source studies. The authors reviewed and edited the output and take full responsibility for the scientific content, numerical values, interpretations, citations, and final manuscript.

References

[1] Applied Technology Council. Seismic evaluation and retrofit of concrete buildings. Technical Report ATC-40, Applied Technology Council, Redwood City, CA, 1996.

[2] Federal Emergency Management Agency. Improvement of nonlinear static seismic analysis procedures. Technical Report FEMA 440, FEMA, Washington, DC, 2005.

[3] European Committee for Standardization. Eurocode 8: Design of structures for earthquake resistance—part 3: Assessment and retrofitting of buildings. Standard EN 1998-3, 2005.

[4] Earthquake Planning and Protection Organization. Greek code for structural interventions (kan.epe.). Technical report, OASP, Athens, Greece, 2011. In Greek.

[5] European Committee for Standardization. Eurocode 6: Design of masonry structures—part 1-1: General rules for reinforced and unreinforced masonry structures. Standard EN 1996-1-1, 2005.

[6] European Committee for Standardization. Eurocode: Basis of structural design. Standard EN 1990, 2002.

[7] European Committee for Standardization. Eurocode 1: Actions on structures—part 1-7: General actions—accidental actions. Standard EN 1991-1-7:2006+A1:2014, 2014.

[8] Uwe Starossek. *Progressive Collapse of Structures*. Thomas Telford, London, 2009. https://doi.org/10.1680/pcos.36109.

[9] Jose M. Adam, Fulvio Parisi, Juan Sagaseta, and Xinzheng Lu. Research and practice on progressive collapse and robustness of building structures in the 21st century. *Engineering Structures*, 173:122–149, 2018. https://doi.org/10.1016/j.engstruct.2018.06.082.

[10] U.S. General Services Administration. Alternate path analysis and design guidelines for progressive collapse resistance. Technical report, GSA, Washington, DC, 2016.

[11] U.S. Department of Defense. Design of buildings to resist progressive collapse. Technical Report UFC 4-023-03, Unified Facilities Criteria, July 2009. Change 4, 10 June 2024. Prepared by the U.S. Army Corps of Engineers, Naval Facilities Engineering Command, and Air Force Civil Engineer Center.

[12] Mehrdad Sasani, M. Bazan, and S. Sagiroglu. Experimental and analytical progressive collapse evaluation of actual reinforced concrete structure. *ACI Structural Journal*, 104(6):731–739, 2007. https://doi.org/10.14359/18955.

[13] Weijian Yi, Qingfeng He, Yan Xiao, and Sashi K. Kunnath. Experimental study on progressive collapse-resistant behavior of reinforced concrete frame structures. *ACI Structural Journal*, 105(4):433–439, 2008. https://doi.org/10.14359/19857.

[14] Kai Qian and Bing Li. Performance of three-dimensional reinforced concrete beam–column substructures under loss of a corner column scenario. *Journal of Structural Engineering*, 139(4):584–594, 2013. https://doi.org/10.1061/(ASCE)ST.1943-541X.0000630.

[15] Manuel Buitrago, Elisa Bertolesi, Juan Sagaseta, Pedro A. Calderón, and José M. Adam. Robustness of reinforced concrete building structures with infill masonry walls: Tests on a purpose-built structure. *Engineering Structures*, 226:111384, 2021. https://doi.org/10.1016/j.engstruct.2020.111384.

[16] M. Buitrago, N. Makoond, J. J. Moragues, J. Sagaseta, and J. M. Adam. Robustness of a full-scale precast building structure subjected to corner-column failure. *Structures*, 52:824–841, 2023. https://doi.org/10.1016/j.istruc.2023.03.146.

[17] Martina Scalvenzi, Sebastiano Gargiulo, Fabio Freddi, and Fulvio Parisi. Impact of seismic retrofitting on progressive collapse resistance of RC frame structures. *Engineering Failure Analysis*, 131:105840, 2022. https://doi.org/10.1016/j.engfailanal.2021.105840.

[18] Yudi Zhang, Xiaowei Cheng, Mengzhu Diao, Yi Li, Hong Guan, and Hailin Sun. FRP retrofit for RC frame substructures against progressive collapse: Scheme optimisation and resistance calculation. *Engineering Structures*, 289:116289, 2023. https://doi.org/10.1016/j.engstruct.2023.116289.

[19] A. de A. Vieira, S.P. Triantafyllou, and D.A. Bournas. Strengthening of rc frame subassemblies against progressive collapse using trm and nsm reinforcement. *Engineering Structures*, 207:110002, 2020. https://doi.org/10.1016/j.engstruct.2019.110002.

[20] Ariel Kousgaard and Ece Erdogmus. Externally applied retrofit system for existing masonry buildings subject to progressive collapse. In Alphose Zingoni, editor, *Research and Applications in Structural Engineering, Mechanics and Computation*, pages 1883–1888, London, UK, 2013. CRC Press / Taylor & Francis Group. ISBN 978-1-138-00061-2. https://doi.org/10.1201/b15963-341.

[21] Ariel Kousgaard and Ece Erdogmus. State-of-the-art review: Analysis and rehabilitation of existing masonry walls against progressive collapse. In Christopher H. Raebel, editor, *AEI 2015: Birth and Life of the Integrated Building*, pages 421–432. American Society of Civil Engineers, 2015. ISBN 9780784479070. https://doi.org/10.1061/9780784479070.037.

[22] Nada Elkady, Levingshan Augusthus Nelson, Laurence Weekes, Nirvan Makoond, and Manuel Buitrago. Progressive collapse: Past, present, future and beyond. *Structures*, 62:106131, 2024. https://doi.org/10.1016/j.istruc.2024.106131.

[23] Uwe Starossek. Progressive collapse of structures: Nomenclature and procedures. *Structural Engineering International*, 16(2):113–117, 2006. https://doi.org/10.2749/101686606777962477.

[24] Franz Knoll and Thomas Vogel. *Design for Robustness*, volume 11 of *Structural Engineering Documents*. International Association for Bridge and Structural Engineering, Zurich, 2009. ISBN 978-3-85748-120-8. https://doi.org/10.2749/sed011.

[25] Bruce R. Ellingwood. Strategies for mitigating risk to buildings from abnormal load events. *International Journal of Risk Assessment and Management*, 7(6/7):828–845, 2007. https://doi.org/10.1504/IJRAM.2007.014662.

[26] Uwe Starossek and Martin Haberland. Approaches to measures of structural robustness. *Structure and Infrastructure Engineering*, 7(7–8):625–631, 2011. https://doi.org/10.1080/15732479.2010.501562.

[27] Giacomo Caredda, Nirvan Makoond, Manuel Buitrago, Juan Sagaseta, Marios Chryssanthopoulos, and Jose M. Adam. Learning from the progressive collapse of buildings. *Developments in the Built Environment*, 15:100194, 2023. https://doi.org/10.1016/j.dibe.2023.100194.

[28] Bassam A. Izzuddin and João Sio. Rational horizontal tying force method for practical robustness design of building structures. *Engineering Structures*, 252:113676, 2022. https://doi.org/10.1016/j.engstruct.2021.113676.

[29] Computers and Structures, Inc. SAP2000 integrated software for structural analysis and design. Version 27.1.0, 2026.